Analyzing the microstructure of a fresh sorbet with X-ray micro-computed tomography: Sampling, acquisition, and image processing

Véronique Masselot, Véronique Bosc, Hayat Benkhelifa

Analyzing the microstructure of a fresh sorbet with X-ray micro-computed tomography: sampling, acquisition, and image processing

Véronique Masselot[a, b], Véronique Bosc[b], Hayat Benkhelifa[a, b]

[a]*Université Paris-Saclay, INRAE, FRISE, 92761, Antony, France*
[b]*Université Paris-Saclay, INRAE, AgroParisTech, SayFood, 91300, Massy, France*

Authors e-mail addresses: veronique.masselot@agroparistech.fr ; veronique.bosc@agroparistech.fr

Corresponding author: Hayat Benkhelifa. hayat.benkhelifa@agroparistech.fr. 16 rue Claude Bernard, 75231, Paris, France.

Abstract

X-ray micro-computed tomography and image processing techniques were used to analyze fresh frozen sorbets at the outlet of a batch freezer. Sorbets made from water and sucrose were visualized and their microstructure was quantified with a resolution of 9 µm. Sodium iodide was confirmed to enhance the contrast between the unfrozen water and ice in sorbets. A thermostated box was employed to keep the samples at frozen state and constant temperature (close to -6 °C) during imaging. A reproducible quantification of size distributions and volume fractions of ice crystals and air bubbles were obtained. Data concerning ice crystals were in agreement with cryo-SEM imaging. Ice crystals represented approximately 50%wt of the product and their mean size was about 60 µm whereas air bubbles represented about 6% of the volume. Finally, X-ray microtomography equipped with a thermostated box was found to be a particularly relevant technique for the analysis of the microstructure of frozen desserts.

Keywords

Fresh sorbet; Microstructure; X-ray micro-computed tomography; image processing.

1. Introduction

A sorbet is a frozen and multiphasic system, with ice crystals and air bubbles as dispersed phase, and an unfrozen cryoconcentrated solution as continuous phase. The freezing step takes place in a scraped surface heat exchanger (SSHE) or freezer, and is the core of the manufacturing process. The mixture of the ingredients, or mix, enters the freezer at approximately 4 °C; ice crystals and air bubbles are generated while the residual matrix containing unfrozen water is continuously concentrated into solids components (i.e. sugars, stabilizers). At the outlet of the exchanger, the sorbet contains an average of 40%wt of ice and air accounts for up to 30% of the volume. The final temperature of the product is between -5 °C and -6 °C (Clarke, 2012; Goff and Hartel, 2013; Stogo, 1998). Ice creams, sorbets and their derivatives are consumed at frozen state, so their sensory properties are strongly dependent on ice crystals features (i.e. number and size). Controlling the amount of air is another important factor as air has also a significant influence on the textural properties of the finished product (Clarke, 2012; Goff and Hartel, 2013). The unfrozen phase, which is cryoconcentrated in sugars and stabilizers during the freezing process, also has an effect on the structural and textural properties of a sorbet. Moreover, the increase in concentration of solids as well as the decrease in temperature influence the viscosity of this unfrozen phase (Masselot et al., 2020); this could have an effect on heat transfers or on diffusion mechanisms necessary for crystallization (Marshall and Goff, 2003).

Microscopic techniques, such as Scanning Electron Microscopy (SEM) or cryo-SEM, Transmission Electron Microscopy (TEM) and optical microscopy were often used to study ice crystals and air bubbles size and distribution in ice creams or sorbets. Several authors studied the effect of formulation with cryo-SEM (Fernandez et al., 2007; Flores and Goff, 1999; Goff et al., 1993; Yuennan et al., 2014) or using thermostated optical microscopic devices (Bolliger et al., 2000; Chang and Hartel, 2002a; Donhowe et al., 1991; Drewett and Hartel, 2007; Faydi et al., 2001). Other microscopic studies focused on the influence of freezing parameters or of storage conditions (Caillet et al., 2003; Cook and Hartel, 2011; Donhowe and Hartel, 1996a, b; Eisner et al., 2005; Russell et al., 1999; Sofjan and Hartel, 2004). Microscopic techniques are powerful as they offer high spatial resolutions; they are useful to visualize the microstructure of frozen foods such as sorbets. However, microscopic techniques also present several drawbacks. First, some of them are invasive and sample preparation sometimes requires denaturing the product for example by substituting the ice crystals with a resin, by

freeze-drying the sample or by isolating the ice crystals by precipitation (Buyong and Fennema, 1988; Chang and Hartel, 2002b; Park et al., 2006; Thiebaud et al., 2002). Furthermore, microscopic technics only allow a two-dimensional visualization of the sample; results are then greatly dependent on the selected plane. The number of particles analyzed has to be sufficiently large to ensure statistically representative results (Hernández Parra et al., 2018). Most of the time, the number of objects per image is not sufficient and several images have to be carefully selected along the sample surface to collect enough representative information. It is often difficult to obtain reliable quantitative data (Guo et al., 2017; Mulot et al., 2019).

Compared to the number of studies cited above, only a small number of recent studies use 3D imaging techniques to analyze the ice and the air phases of frozen desserts. In particular, X-ray micro-computed tomography (X-ray micro-CT) is well adapted to the typical size of the frozen food microstructures (above 10 µm). This method measures the level of attenuation of X-rays of the different materials constituting of a sample; this attenuation coefficient is a function of the atomic number, the density and the thickness of the material (Mousavi et al., 2005). The sample is placed on a rotating stage between an X-ray source and a detector and radiographs are acquired from different angles. Hundreds of 2D slices are collected. Finally, 3D images are reconstructed from these radiographies and can be treated with several image processing techniques to give access to the 3D microstructure (Landis and Keane, 2010). X-ray micro-CT can be non-invasive and non-destructive even if most of the studies published about the microstructure of frozen foods was restricted to ambient temperature by using a prior freeze drying step, which is an indirect and destructive technique (Kobayashi et al., 2014; Mousavi et al., 2005; Mousavi et al., 2007; Mulot et al., 2019; Ullah et al., 2014; Zhao and Takhar, 2017). In the case of ice cream or sorbet, freeze drying is not applicable since the product would be totally melted; therefore the sample has to be observed directly at frozen state. Van Dalen (2012) successfully applied this technique to observe air bubbles in ice cream by coupling X-ray micro-CT with a specific Peltier cooling system to keep the sample down to -20 °C. The investigation of air microstructure using X-ray micro-CT was found to be particularly adapted since the contrast between air and condensed materials is high. Pinzer et al. (2012) studied the effect of a change in temperature during storage of ice cream on the size of ice crystals and air bubbles; the authors used a laboratory X-ray source placed in a cold lab which temperature oscillated between -20 °C and -8 °C. They also showed that the addition of approximately 3% of sodium iodide as a

contrast agent allowed enhancing the phase contrast between the two aqueous phases of ice cream (i.e. ice phase and unfrozen phase). Other authors described the influence of temperature cycles on the size and morphology of ice crystals and air bubbles in ice cream using in-line phase contrast synchrotron X-ray tomography technique in order to enhance the contrast between liquid water and ice and improve image quality and resolution (Guo et al., 2018; Guo et al., 2017; Mo et al., 2019; Mo et al., 2018). These authors developed a complex cold stage that was incorporated into the synchrotron line. These interesting studies established the possibility of analyzing frozen desserts with X-ray micro-CT. Since commercial micro-CT devices are adapted for ambient temperature imaging and not equipped with thermostated stage, specific tools have been developed to maintain the samples at frozen state during imaging; they are powerful but also complex and difficult to reproduce. Therefore, the use of a simple thermostated system which would be easy to reproduce is a challenge. Furthermore, the previous articles also contributed to a better understanding of the complex mechanisms occurring during the storage of ice cream: indeed, when the temperature fluctuates, recrystallization and coalescence of air bubbles occur. Imaging a fresh frozen dessert using micro-CT directly after the freezing process would allow understanding the influence of this process or of the formulation on the initial formation of the microstructure and would be innovative. However, such an analysis is difficult since the product is particularly sensitive at these temperatures (i.e. about -6 °C). Finally, describing in details methodologies used for image processing is another challenge since the publications rather referred to other papers specific to image analysis.

The main objective of the present study was to apply X-ray micro-CT to visualize and quantify ice crystals and air bubbles in a fresh sorbet containing water, sugar and a contrast agent. The goals of this work were to i) maintain the sorbet at constant temperature and frozen state during imaging by using a thermostated box; this box was simple to use and easy to reproduce ii) establish a reliable and reproducible methodology of micro-CT acquisition to visualize the microstructure of a fresh sorbet directly after its freezing in a batch freezer; iii) develop reliable image processing methods to analyze ice crystals and air bubbles; iv) obtain quantitative data about the microstructure confirmed with cryo-SEM imaging.

2. Materials and methods

2.1.Preparation and freezing of the sorbet mixes

A simple formulation of sorbet containing water and sucrose was studied. Sucrose was purchased from Béghin Say®. The sugar concentration was set at 25%wt to represent that of an industrial sorbet mix (Clarke, 2012; Goff and Hartel, 2013). Sorbet mixes were prepared with deionized water (conductivity 17 µS.m-1) to ensure constant quality of water. Mixes were obtained by dispersing sucrose in water at ambient temperature under agitation using a magnetic stirrer. They were then cooled at 4 °C for at least 12 hours before freezing. In order to improve the contrast between the ice crystals and the unfrozen residual solution during micro-CT imaging (Pinzer et al., 2012), 30g of sodium iodide (NaI purchased from Merck®, CAS Number 7681-82-5) was added per kilogram of mix just before the freezing step. Mixes without sodium iodide were also prepared to study its effect on phase contrast.

The mixes (800 mL) were frozen in a batch domestic scraped surface heat exchanger (Magimix® Gelato Expert); it was equipped with two scrapping blades rotating at about 50 rpm. The temperature of the sorbet was monitored regularly during freezing with a penetration thermometer (accuracy 0.5 °C; Testo 104, Testo, Forbach, France). Since the objective of the present study was to observe the microstructure of a sorbet at the end of the freezing process in a SSHE, freezing was stopped when the sorbet temperature reached -6 °C corresponding to classical temperatures encountered for sorbets at the outlet of an industrial scraped surface heat exchanger. The freezing time to reach this temperature was about 25 minutes whatever the formulation of the mix (i.e. with or without NaI). To ensure the same freezing conditions and thermal history of each sample, a batch was carried out per sample.

2.2.X-ray micro-computed tomography

2.2.1. Sampling

Once the desired temperature in the freezer was reached, a pre-cooled plastic straw (6 mm of diameter, 2.3 cm long) was inserted in the center of the freezer to extract a small quantity of fresh frozen sorbet. The most efficient geometry to scan is a cylinder; the use of straws was therefore a good compromise. The accuracy of the tomographic analysis is related to the distance between the sample and the X-ray source, which is limited by the size of the sample. A small sample close to the

X-ray source enables high accuracy. To ensure that the temperature of the sorbet was maintained at about -6 °C during the tomographic scan, the frozen samples were placed in a specific thermostated box designed and manufactured in our laboratory with photopolymer resins thanks to a 3D printer (Formlabs®, Form 2). This is shown in figure 1.

The first part of the device consisted of a cylindrical double jacket box (2 cm of diameter, 2.5 cm long) made of transparent resin (Clear resin FLGPCL04, Formlabs®) and containing a phase change material (PCM) at -6 °C (E-6, Cristopia Energy Systems®) gelled with a 2%wt commercial gum blend (Germantown Premium IC Blend, Danisco). The PCM had two functions: it kept the frozen sample at the right temperature during scanning and was used as a melting indicator if the temperature rose above -6 °C. Another cylindrical double jacket box (3.5 cm of diameter, 6 cm long) made of gray resin (Grey resin FLGPGR04) was printed to surround the first box; it was filled with an expansive insulating foam. The thermostated box was stored in a freezer at -10 °C before micro-CT analyzes.

2.2.2. Image acquisition of frozen samples

The sample conditioned in the thermostated box was positioned on the rotating stage of the X-ray micro-CT (DeskTom 130®, RX Solution, Chavanod, France) as close as possible to the X-ray source so that its middle part was analyzed with a voxel resolution of 9µm. The system was operating at an X-ray tube voltage of 50 kV and a current intensity of 160 µA.

A preliminary thermal study of the sample during a tomographic analysis was carried out to determine the maximal possible scanning time without sample melting. Three calibrated thermocouples (type T) were used: one was placed in the center of the straw filled with sorbet, another one was placed in the PCM material and the third one measured the temperature of the air in the micro-CT close to the thermostated box. The temperature was recorded during 30 minutes; it allowed setting the CT scan duration (see section 3.1).

Imaging the rotating sample allowed obtaining attenuation profiles of the entire sorbet sample according to the angle of acquisition (i.e. projections). Tomographic reconstruction was then applied to obtain 2D slices and the 3D volume of the sorbet from these projections. XAct 2® software (RX Solution, Chavanod, France) was used for the reconstruction operation using a filtered back-projection algorithm; this is the most popular reconstruction algorithm used at present in CT applications (Al

Hussani and Ali Al Hayani, 2014). A filter was then applied to correct ring artefacts which result from a non-linear response of the micro-CT detector (Hseih, 2009). More than 1300 slices were provided in 16-bits resolution from the volume reconstruction (i.e. grayscale levels from 0 to 65536).

2.2.3. Image processing and quantitative analysis of air bubbles and ice crystals

After the 3D volume reconstruction, data were loaded on Avizo 2019.1® software (Thermo Fisher Scientific, Waltham, USA) for image analysis. In order to reduce the processing time to a few minutes, a cubic sub-volume (360 x 360 x 360 voxels equivalent to a 3.2 mm side cube) was cropped at the center of the reconstructed 3D volume. This sub-volume was confirmed to be higher than the Representative Elementary Volume defined for typical microstructure sizes encountered in frozen foods (Vicent et al., 2017). The three phases of the sorbet (i.e. air, ice, unfrozen matrix containing the contrast agent) having different densities, they are expected to demonstrate different gray levels. The aim of image processing is then to create separations between the particles of the phase of interest (i.e. air phase or ice phase) in order to individualize them and then obtain the quantitative data. Depending on the characteristics of the phase and in particular its homogeneity in terms of gray level, several image processing options are available for further treatment (User's Guide Avizo Software 2019). The treatments for image processing of the air and ice phases are presented in the results section. Once the elements of interest were isolated and separated from each other, it was possible to extract quantitative information about each of the particles. Data were then exported to analyze ice crystals or air bubbles size distribution and volume fraction of these two phases. Equivalent diameter of each particle was calculated as described by equation 1. In 3D geometry, it represents the diameter of a sphere having the same volume as the particle.

$$d_V = \sqrt[3]{\frac{6V}{\pi}} \qquad (1)$$

where V is the volume of the particle.

The resolution limit of micro-CT analysis to identify structures is commonly assumed to be between two and three voxels size (Pinzer et al., 2012; Vicent et al., 2017) , in the case of the present study this corresponds to particles having equivalent diameters larger than 20 µm. Therefore objects smaller than 20 µm were excluded from the analysis described below.

The volume fraction of ice in the sample without air φ_i was calculated according to equation 2.

$$\varphi_i = \frac{V_{i0}}{V_{i0}+V_m} \quad (2)$$

where V_{i0} is the initial volume fraction of ice with air (%) and V_m the initial volume fraction of the unfrozen matrix with air (%). The mass fraction of ice X_i is then obtained with equation 3.

$$X_i = \frac{\varphi_i * \rho_i}{\rho_S} \quad (3)$$

where ρ_i is the volumetric mass density of ice and ρ_S the volumetric mass density of the sorbet at a given temperature.

At the end of the image processing, a three dimensional view of the phase of interest was obtained. Three sorbets samples were analyzed using X-ray micro-CT.

2.3.Cryo-scanning electron microscopy

Cryo-SEM measurements were carried out in an external laboratory equipped with scanning electron microscopy (Electron Microscopy Facility, IBPS, Paris, France), in order to compare imaging results to those obtained with the microtomographic method. In order to avoid melting or modification of the sorbet, the freezer was installed in this laboratory in the vicinity of the cryo-SEM facility and mixes were frozen on site. The fresh frozen sorbet was taken in a plastic straw and directly immersed in liquid nitrogen. The straw was then cut and a fragment of sorbet was extracted for cryofracture. Fractured surfaces were observed using cryo-SEM (GeminiSEM 500, Zeiss) at -120 °C, the pressure in the equipment was 1.6×10^{-4} Pa. The accelerating voltage was 3.00 kV or 0.790 kV and the magnification varied from x13 to x10 000. The pixel resolution was from 9 µm to 11 nm. Image processing was also performed using Avizo 2019.1®; manual segmentation and separation of the particles were performed. Equivalent diameters of particles were obtained with the equation 4. In 2D, it represents the diameter of a disk having the same area as the particle.

$$d_s = \sqrt{\frac{4*S}{\pi}} \quad (4)$$

where *S* is the surface of the particle.

Since the availability of the cryo-SEM facility was limited, only one sample could be analyzed with cryo-SEM. However, the entire cryo-fractured area was imaged so as to visualize a sufficient number of objects (more than 200) for image analysis.

3. Results and discussion

3.1.Temperature of sorbets during micro-CT measurements

The temperature of the sorbet in the thermostated box and of the PCM which surrounds the sorbet was recorded during a tomographic imaging (Figure 2) in order to ensure that the sorbet remained frozen and at a temperature close to -6 °C during the tomographic scanning. This study was also intended to fix the imaging duration. The temperature of the air in the micro-CT device was stable at around 21 °C (data not shown). The sorbet was imaged at a temperature between -7 °C and -8 °C; this temperature was maintained during about 20 minutes in the thermostated box as illustrated by the red arrow in Figure 2., Therefore, the thermostated box demonstrated its ability to maintain sorbets at frozen state and at constant temperature during a micro-CT imaging if the scanning time is sufficiently short. In the case of the present study, the duration of the micro-CT scanning was set at 12 minutes.

3.2.Effect of sodium iodide on the contrast of X-rays radiographs

Micro-CT images after the reconstruction step for sorbet samples without and with NaI are shown respectively in Figure 3 (a) and (b). Air appeared in black, the ice phase and the unfrozen matrix were in gray. As expected, the visual differentiation of the two aqueous phases was much easier in the sample containing NaI: ice was in dark gray, unfrozen matrix was in light gray and surrounded the ice crystals and the air bubbles (Pinzer et al., 2012). Figures 3 (c) and (d) present the grayscale histograms obtained for the sorbet samples without and with NaI. The histogram without NaI was unusable since a single Gaussian peak was obtained containing voxels from both the ice phase and the unfrozen phase. On the contrary, the histogram obtained with NaI showed two separate peaks of gray levels making it possible to separate the ice phase and the unfrozen phase. These peaks overlapped each other; the crossing value was defined as the thresholding value. The histograms also revealed that the voxels of the air phase had different gray levels with or without NaI (respectively from 17500 to 26000 and from 0 to 17500). The use of the contrast agent could cause a greater beam

hardening when X-rays passed through the unfrozen phase, and since the reconstruction parameters were applied to the entire sample, this had an effect on the attenuation levels and therefore on the gray levels of all the phases, including the air phase. Finally, with NaI, the air phase consisted of voxels with gray intensities from 17500 to 26 000, the ice fraction contained the voxels having gray levels from 26000 to 36000 and the other voxels were attributed to the unfrozen solution. These values were obtained for the three samples containing NaI and were applied for segmentation (see section 3.3).

3.3.Image analysis of frozen samples

3.3.1. Air bubbles

As shown in figure 3(b), the air phase was homogeneously black. The images were segmented and all the voxels having grayscale intensities between 0 and 26000 were attributed to the air phase. Only the air phase was kept for further image processing and the grayscale images were binarized: all the voxels being part of the air phase were colored in blue (Figure 4(a)). A distance map was then calculated from the binarized images, it allowed determining the dimensions of the particles. The most inner regions within objects were detected in order to determine the centers of the air bubbles. Then, the objects in contact with each other were separated using a classical watershed algorithm. The bubbles in contact with the sub-volume walls were suppressed with a borderkill algorithm and the remaining particles were labeled in order to be individualized. Each bubble was individually color-rendered for a better visualization. The final result is shown in Figure 4(b). The air phase was properly segmented and the bubbles were well separated from each other. Figure 4(c) represents the 3D visualization of the air bubbles distribution, it shows few air bubbles and sizes and shapes seem to be heterogeneous. In the literature (Guo et al., 2018; Guo et al., 2017; Mo et al., 2018; Pinzer et al., 2012; Van Dalen, 2012), 3D imaging of ice cream show more numerous and more homogeneous air bubbles in terms of size and shape. In these studies, the ice cream was produced in a continuous SSHE, a freezer equipped with nozzles to control the incorporation of air under pressure. The fast rotation of the scrapping blades (until 500 rpm) distributes the air homogenously as small bubbles. Moreover, the complex formulation of ice creams (i.e. containing emulsifiers with interfacial properties) analyzed in these studies can explain a better stabilization of air bubbles.

Using cryo-SEM, only one or two air bubbles were visualized on the images (data not shown), therefore it was not possible to analyze the air bubbles with this technique. As explained previously, the micro-CT images revealed only a small quantity of air bubbles in the sorbet samples; therefore it could be possible that no air bubble was present in the fractured plane visualized in cryo-SEM. Furthermore, unlike with micro-CT images, the contrast and gray level difference between air particles and ice was not large on the cryo-SEM images. It is therefore possible that some air bubbles were mistaken for ice crystals unintentionally.

3.3.2. Ice crystals

The raw micro-CT images after the reconstruction step (Figure 5(a)) revealed that the ice phase (intermediate gray) was not homogeneous in terms of gray level. This was probably due to the cupping effect: X-rays interact with the particles (i.e. ice crystals) when they pass through the sample. Each point of the crystal behaves like a source of secondary radiation emitting in all directions and then towards the detector which also receives X-rays coming from the source. Secondary radiation is particularly intense from the inner regions of the particles; it induces an overestimation of the X-rays received by the detector and therefore an underestimation of the attenuation of X-rays by the central region of the particles. Finally, the inner region of the particles appears darker (Wils, 2011; Yang et al., 2020). The results obtained by performing the same image processing on the ice phase as for the air phase (see section 3.3.1) are shown in Figure 5(b). With this treatment, the ice phase was directly segmented (i.e. binarized) and the position of the central regions of the crystals given by the cupping effect was lost. The results showed that this treatment method was not suitable for the analysis of ice crystals. The adjacent crystals were not separated and the image rather showed clusters of ice crystals.

Since the heterogeneity of the ice phase allowed determining the inner regions of adjacent ice crystals, an H-extrema watershed algorithm were applied on grayscale images (Figure 5(c)). This algorithm combined the marking of darker regions as inner regions (H-maxima) and the watershed operation which allowed separating the particles from each other and obtaining their edges. Independently of these operations, grayscale images were segmented as explained in the section 3.2; voxels having gray levels from 26000 to 36000 were isolated and marked as the ice phase. The edges of the crystals were subtracted from this binarized image, the ice crystals were then separated from each other and individually color-rendered. As for air bubbles, objects in contact with the sub-volume

303 walls were suppressed (Figure 5(d)). Figure 5(e) represents the 3D visualization of the ice crystals; on
304 this figure the crystals appear clearly small and numerous.

305 Ice crystals were also clearly visible using cryo-SEM (Figure 6(a)). Three images were
306 segmented (Figure 6(b)) and finally, 219 ice crystals were analyzed. By comparing Figure 6(b) and
307 Figure 6(c) obtained by micro-CT imaging, it appears that the number and size of ice crystals were of
308 the same order of magnitude. The shape of the ice crystals seemed to match even if the ice crystals
309 were more rounded in the case of the cryo-SEM image. This can be explained by the differences in
310 the image processing techniques but more probably by the spatial resolution of both devices that is
311 significantly higher in the case of cryo-SEM; this explains that pixels are not distinguished using cryo-
312 SEM. Quantitative data from cryo-SEM pictures were obtained for comparison with micro-CT data;
313 they are discussed in the section 3.4.

314 ## 3.4.Quantitative analysis of sorbet microstructure

315 ### 3.4.1. Analysis of the air phase

316 The cumulative distribution of air cells equivalent diameters in the three samples analyzed
317 using X-ray micro-CT were plotted in figure 7. The results reflected the good reproducibility of the
318 analysis protocol (i.e. formulation, freezing, sampling, micro-CT analysis, image processing). The air
319 bubbles sizes were distributed between 20 and 585 µm, the width of the distribution illustrated the
320 heterogeneity of the bubbles size. As cryo-SEM did not allow distinguishing air bubbles, it was not
321 possible to compare the two techniques for the air phase.

322 The mean and median equivalent diameters, the volume fraction of the air phase and the
323 number of air bubbles were calculated. The volume fraction of air, equal to 5.6 ± 0.7%, was found to
324 be smaller than the amount of air generally encountered in a commercial sorbet (30%). This was not
325 surprising regarding the 3D rendering of air bubbles (Figure 4(c)), the composition and the freezing
326 equipment used for this study. The mean and the median bubbles size (equivalent diameter) were
327 different, respectively 123.4 µm and 105.1 µm, and both admitted a significant standard deviation of
328 the order of 10%. This confirms the heterogeneity of the air bubbles in terms of size within the same
329 sample as between several different samples. Guo et al. (2017) observed using micro-CT air cells in a
330 commercial ice cream at -15 °C; they obtained a mean bubble size of 36 µm. Industrial ice creams

331 being obtained via a continuous freezer and their complex composition comprising surfactant
332 molecules, it was not surprising that this size was smaller than that obtained in the present study.
333 These authors also obtained a significant standard deviation of the order of 50%. Using cryo-SEM, the
334 authors found a mean bubble size equal to 41 µm with an important standard deviation of about 50%.

335 ### 3.4.2. Analysis of ice crystals

336 The cumulative distribution of ice crystals equivalent diameters in the three samples analyzed
337 using X-ray micro-CT and in the sample analyzed using cryo-SEM are reported in figure 8. The results
338 illustrated the repeatability of the micro-CT analysis for the study of ice crystals as the three curves
339 were perfectly superimposed. Using this technique, it was found that the ice crystals equivalent
340 diameters were comprised between 20 µm and 158 µm. By comparing these results with those
341 obtained with cryo-SEM, the distribution was in the same order of magnitude (between 18 µm and 134
342 µm) while slightly shifted to smallest crystal sizes. This is probably due to the small number of crystals
343 analyzed (219) and the manual segmentation technique used.

344 Mean and median equivalent diameters, volume and mass fractions of the ice phase and the
345 number of particles obtained with micro-CT and with cryo-SEM are reported in table 1. Whatever the
346 experimental technique used, the mean and the median values of the ice crystal size were close; the
347 distribution of the ice crystals size was homogeneous in the sample. The mean equivalent diameter of
348 ice crystals was about 63 µm for micro-CT and 56 µm for Cryo-SEM. The low standard deviations
349 (about 2%) confirmed the small dispersion of ice crystal size between replicates as well as the good
350 repeatability of the micro-CT analyzes. Mo et al. (2019) analyzed the coarsening effect in a frozen
351 sorbet containing 30% of sucrose submitted to several thermal cycling and cooling rates. At -6 °C,
352 they found that according to these parameters, the mean size of the ice crystals was between 30 and
353 70 µm which is close to the values obtained in the present study.

354 The ice volume fraction without air in the sorbet was equal to 58%. Cerecero Enriquez (2003)
355 established the liquidus curve of a solution containing 25% of sucrose by using DSC. At -6 °C the
356 corresponding ice mass fraction was equal to 44.4%. In the present study, the mean mass fraction
357 was estimated at about 48%. These values are close; the small difference can be explained by the
358 uncertainty of the measurement of the sorbet temperature before micro-CT imaging. This result could
359 also indicate that the amount of sodium iodide used in this study did not have a significant influence on

360 the ice fraction formed during the freezing of a sorbet containing water and sucrose. This was not
361 studied in the literature, therefore other analyzes would be relevant to confirm this observation.

362 Micro-CT and cryo-SEM ice crystals equivalent diameters were in the same order of
363 magnitude; this result allowed validating the micro-CT analysis from sampling to image processing.
364 The small difference between the two methods can be explained by the different number of crystals
365 analyzed (respectively about 78000 versus 220). It should also be kept in mind that the determination
366 of the mean equivalent diameter referred respectively to the volume (see equation 1) or to the surface
367 (see equation 4). Other explanations could be that some small and round particles were mistaken for
368 ice crystals on cryo-SEM pictures. Finally, manual segmentation was delicate.

Table 1. Ice crystals quantitative data. ±values correspond to standard deviations.

	Mean of the 3 CT samples	Cryo-SEM sample
Mean equivalent diameter (µm)	62.8 ± 1.4	56.5
Median equivalent diameter (µm)	61.8 ± 1.3	53.4
Volume fraction of the phase (%)	54.7 ± 2.8	---
Volume fraction of the phase without air (equation 2) (%)	58.0 ± 2.6	
Mass fraction of the phase (%)	48.3 ± 2.1	---
Number of particles	77 935 ± 1 826	219

369 ## 4. Conclusions and perspectives

370 Sorbet mixes containing water and 25%wt of sucrose were frozen and analyzed by X-ray
371 microtomography directly after the freezing step. A desktop micro-CT device was used, and a
372 thermostated box was successfully applied; this system is simple to use and makes the experimental
373 methodology easy to reproduce. The protocol allowed a reproducible and nondestructive analysis of a
374 complex and triphasic frozen product. X-ray microtomography showed to be a powerful tool enabling
375 the scanning of hundreds of images per analysis. In this study, more than 1300 slices were processed
376 per acquisition and an effective separation of the 2 phases of interest (ice crystals and air bubbles)
377 was carried out. The data collected gave the desired information about the frozen phase and the air
378 phase (volume and mass fractions, mean and median equivalent diameters of the particles, size
379 distributions and spatial distributions thanks to the 3-dimensional visualization). Results were in
380 agreement with the literature, the differences being explained by the composition of the mixes and by
381 the freezing process used. Qualitative and quantitative results about ice crystals were confirmed with
382 cryo-SEM measurements. As a result, X-ray microtomography equipped with this thermostated box

seems to be a particularly appropriate technique for the analysis of the microstructure of frozen desserts.

For future studies of frozen microstructure of sorbets, it will be necessary to control the thermal behavior of sorbet mixes containing a contrast agent (i.e. sodium iodide) in order to confirm its possible influence on the formation and growth of ice crystals during freezing process. Since NaI might have effects on the microstructure of sorbets (i.e. size and quantity of bubbles or crystals), it also would be relevant to analyze sorbets containing several concentrations of sodium iodide. It will also be necessary to validate results concerning air bubbles using cryo-SEM. The amount of air in the sample has to be sufficiently high to be visible with this technique. Then, it would be appropriate to add a surfactant to the mix (such as hydroxypropylmethylcellulose which is a stabilizer commonly used in the formulation of sorbets). The next step of this work is to extend the use of this technique to the characterization of sorbets having a more complex composition (in particular sorbets containing stabilizers such as galactomannans, cellulose derivatives, or mixtures of several stabilizers) in order to study the effect of formulation on the crystallization of sorbets. This information would lead to a better understanding of the effect of stabilizers on the initial formation of the microstructure during the freezing step, before hardening and storage. This will also help to understand and predict to what extent the behavior of stabilizers during the freezing step influences the final stability of sorbets and which stage of the process or the storage have the greatest impact on the microstructure. Finally, the methodology developed can be applied for the study of the microstructure of other frozen foods.

Funding

This work was supported by the French Ministry of Higher Education, Research and Innovation.

References

Al Hussani, M., Ali Al Hayani, M., (2014). The Use of Filtered Back projection Algorithm for Reconstruction of tomographic Image. 151-156.

Bolliger, S., Wildmoser, H., Goff, H.D., Tharp, B.W., (2000). Relationships between ice cream mix viscoelasticity and ice crystal growth in ice cream. *International Dairy Journal,* 10(11), 791-797. https://doi.org/10.1016/s0958-6946(00)00108-4

Buyong, N., Fennema, O., (1988). Amount and size of ice crystals in frozen samples as influenced by hydrocolloids. *Journal of Dairy Science,* 71(10), 2630-2639. https://doi.org/10.3168/jds.S0022-0302(88)79856-2

Caillet, A., Cogné, C., Andrieu, J., Laurent, P., Rivoire, A., (2003). Characterization of ice cream structure by direct optical microscopy. Influence of freezing parameters. *LWT - Food Science and Technology,* 36(8), 743-749. https://doi.org/10.1016/S0023-6438(03)00094-X

Cerecero Enriquez, R., (2003). Etude des écoulements et des transferts thermiques lors de la fabrication d'un sorbet à l'échelle du pilote et du laboratoire. Institut National Agronomique Paris Grignon, Paris, p. 161.

Chang, Y., Hartel, R.W., (2002a). Development of air cells in a batch ice cream freezer. *Journal of Food Engineering,* 55(1), 71-78. https://doi.org/10.1016/S0260-8774(01)00243-6

Chang, Y., Hartel, R.W., (2002b). Stability of air cells in ice cream during hardening and storage. *Journal of Food Engineering,* 55(1), 59-70. https://doi.org/10.1016/S0260-8774(01)00242-4

Clarke, C., (2012). *The Science of Ice Cream* (2nd ed). RSCPublishing, Cambridge.

Cook, K.L.K., Hartel, R.W., (2011). Effect of freezing temperature and warming rate on dendrite break-up when freezing ice cream mix. *International Dairy Journal,* 21(6), 447-453. https://doi.org/10.1016/j.idairyj.2011.01.007

Donhowe, D.P., Hartel, R.W., (1996a). Recrystallization of ice during bulk storage of ice cream. *International Dairy Journal,* 6(11), 1209-1221. https://doi.org/10.1016/S0958-6946(96)00030-1

Donhowe, D.P., Hartel, R.W., (1996b). Recrystallization of ice in ice cream during controlled accelerated storage. *International Dairy Journal,* 6(11), 1191-1208. https://doi.org/10.1016/S0958-6946(96)00029-5

Donhowe, D.P., Hartel, R.W., Bradley, R.L., (1991). Determination of Ice Crystal Size Distributions in Frozen Desserts. *Journal of Dairy Science,* 74(10), 3334-3344. https://doi.org/10.3168/jds.S0022-0302(91)78521-4

Drewett, E.M., Hartel, R.W., (2007). Ice crystallization in a scraped surface freezer. *Journal of Food Engineering,* 78(3), 1060-1066. https://doi.org/10.1016/j.jfoodeng.2005.12.018

Eisner, M.D., Wildmoser, H., Windhab, E.J., (2005). Air cell microstructuring in a high viscous ice cream matrix. *Colloids and Surfaces A: Physicochemical and Engineering Aspects,* 263(1), 390-399. https://doi.org/10.1016/j.colsurfa.2004.12.017

Faydi, E., Andrieu, J., Laurent, P., (2001). Experimental study and modelling of the ice crystal morphology of model standard ice cream. Part I: Direct characterization method and experimental data. *Journal of Food Engineering,* 48(4), 283-291. https://doi.org/10.1016/S0260-8774(00)00168-0

Fernandez, P.P., Martino, M.N., Zaritzky, N.E., Guignon, B., Sanz, P.D., (2007). Effects of locust bean, xanthan and guar gums on the ice crystals of a sucrose solution frozen at high pressure. *Food Hydrocolloids,* 21(4), 507-515. https://doi.org/10.1016/j.foodhyd.2006.05.010

Flores, A.A., Goff, H.D., (1999). Ice crystal size distributions in dynamically frozen model solutions and ice cream as affected by stabilizers. *Journal of Dairy Science,* 82, 1399-1407. https://doi.org/10.3168/jds.S0022-0302(99)75366-X

Goff, H.D., Caldwell, K.B., Stanley, D.W., Maurice, T.J., (1993). The influence of polysaccharides on the glass-transition in frozen sucrose solutions and ice-cream. *Journal of Dairy Science,* 76(5), 1268-1277. https://doi.org/10.3168/jds.S0022-0302(93)77456-1

Goff, H.D., Hartel, R.W., (2013). *Ice cream* (7th ed. ed). Springer, New York.

Guo, E., Kazantsev, D., Mo, J., Bent, J., Van Dalen, G., Schuetz, P., Rockett, P., StJohn, D., Lee, P.D., (2018). Revealing the microstructural stability of a three-phase soft solid (ice cream) by 4D synchrotron X-ray tomography. *Journal of Food Engineering,* 237, 204-214. https://doi.org/10.1016/j.jfoodeng.2018.05.027

Guo, E., Zeng, G., Kazantsev, D., Rockett, P., Bent, J., Kirkland, M., Van Dalen, G., Eastwood, D.S., StJohn, D., Lee, P.D., (2017). Synchrotron X-ray tomographic quantification of microstructural evolution in ice cream-a multi-phase soft solid. *RSC Advances,* 7(25), 15561-15573. https://doi.org/10.1039/c7ra00642j

Hernández Parra, O.D., Ndoye, F.T., Benkhelifa, H., Flick, D., Alvarez, G., (2018). Effect of process parameters on ice crystals and air bubbles size distributions of sorbets in a scraped surface heat exchanger. *International Journal of Refrigeration,* 92, 225-234. https://doi.org/10.1016/j.ijrefrig.2018.02.013

Hseih, J., (2009). *Computed Tomography - Principles, Design, Artifacts and Recent Advances*.
Kobayashi, R., Kimizuka, N., Suzuki, T., Watanabe, M., (2014). Effect of supercooled freezing methods on ice structure observed by X-ray CT, *Refrigeration Science and Technology*, pp. 392-396.
Landis, E.N., Keane, D.T., (2010). X-ray microtomography. *Materials Characterization,* 61(12), 1305-1316. https://doi.org/10.1016/j.matchar.2010.09.012
Marshall, R.T., Goff, D., (2003). Formulating and manufacturing ice cream and other frozen desserts. *Food Technology,* 57(5), 32-45.
Masselot, V., Benkhelifa, H., Cuvelier, G., Bosc, V., (2020). Rheological properties of stabilizers at low temperatures in concentrated sucrose solutions. *Food Hydrocolloids,* 103, 105691. https://doi.org/10.1016/j.foodhyd.2020.105691
Mo, J., Groot, R.D., McCartney, G., Guo, E., Bent, J., van Dalen, G., Schuetz, P., Rockett, P., Lee, P.D., (2019). Ice crystal coarsening in ice cream during cooling: A comparison of theory and experiment. *Crystals,* 9(6). https://doi.org/10.3390/cryst9060321
Mo, J., Guo, E., Graham McCartney, D., Eastwood, D.S., Bent, J., Van Dalen, G., Schuetz, P., Rockett, P., Lee, P.D., (2018). Time-resolved tomographic quantification of the microstructural evolution of ice cream. *Materials,* 11(10). https://doi.org/10.3390/ma11102031
Mousavi, R., Miri, T., Cox, P.W., Fryer, P.J., (2005). A Novel Technique for Ice Crystal Visualization in Frozen Solids Using X-Ray Micro-Computed Tomography. *Journal of Food Science,* 70(7), 437-442. https://doi.org/10.1111/j.1365-2621.2005.tb11473.x
Mousavi, R., Miri, T., Cox, P.W., Fryer, P.J., (2007). Imaging food freezing using X-ray microtomography. *International Journal of Food Science and Technology,* 42(6), 714-727. https://doi.org/10.1111/j.1365-2621.2007.01514.x
Mulot, V., Fatou-Toutie, N., Benkhelifa, H., Pathier, D., Flick, D., (2019). Investigating the effect of freezing operating conditions on microstructure of frozen minced beef using an innovative X-ray micro-computed tomography method. *Journal of Food Engineering,* 262, 13-21. https://doi.org/10.1016/j.jfoodeng.2019.05.014
Park, S.-H., Hong, G.-P., Kim, J.-Y., Choi, M.-J., Min, S.-G., (2006). The influence of food hydrocolloids on changes in the physical properties of ice cream. *Food Science and Biotechnology,* 15(5), 721-727.
Pinzer, B.R., Medebach, A., Limbach, H.J., Dubois, C., Stampanoni, M., Schneebeli, M., (2012). 3D-characterization of three-phase systems using X-ray tomography: tracking the microstructural evolution in ice cream. *Soft Matter,* 8(17), 4584-4594. https://doi.org/10.1039/C2SM00034B
Russell, A.B., Cheney, P.E., Wantling, S.D., (1999). Influence of freezing conditions on ice crystallisation in ice cream. *Journal of Food Engineering,* 39(2), 179-191. https://doi.org/10.1016/S0260-8774(98)00161-7
Sofjan, R.P., Hartel, R.W., (2004). Effects of overrun on structural and physical characteristics of ice cream. *International Dairy Journal,* 14(3), 255-262. https://doi.org/10.1016/j.idairyj.2003.08.005
Stogo, M., (1998). *Ice cream and fozen desserts: a commercial guide to production and marketing*. John Wiley & Sons, Hoboken.
Thiebaud, M., Dumay, E.M., Cheftel, J.C., (2002). Pressure-shift freezing of o/w emulsions: influence of fructose and sodium alginate on undercooling, nucleation, freezing kinetics and ice crystal size distribution. *Food Hydrocolloids,* 16(6), 527-545. https://doi.org/10.1016/s0268-005x(01)00133-3
Ullah, J., Takhar, P.S., Sablani, S.S., (2014). Effect of temperature fluctuations on ice-crystal growth in frozen potatoes during storage. *LWT - Food Science and Technology,* 59(2P1), 1186-1190. https://doi.org/10.1016/j.lwt.2014.06.018
Van Dalen, G., (2012). A Study of Bubbles in Foods by X-RayMicrotomography and Image Analysis. *Microscopy and Analysis*, S8-S12.
Vicent, V., Verboven, P., Ndoye, F.-T., Alvarez, G., Nicolaï, B., (2017). A new method developed to characterize the 3D microstructure of frozen apple using X-ray micro-CT. *Journal of Food Engineering,* 212, 154-164. https://doi.org/10.1016/j.jfoodeng.2017.05.028
Wils, P., (2011). Artefacts correction in X-ray cone-beam computed tomography CBCT. INSA de Lyon.

Yang, F., Zhang, D., Zhang, H., Huang, K., (2020). Cupping artifacts correction for polychromatic X-ray cone-beam computed tomography based on projection compensation and hardening behavior. *Biomedical Signal Processing and Control,* 57, 101823. https://doi.org/10.1016/j.bspc.2019.101823
Yuennan, P., Sajjaanantakul, T., Goff, H.D., (2014). Effect of okra cell wall and polysaccharide on physical properties and stability of ice cream. *Journal of food science,* 79(8), 1522-1527. https://doi.org/10.1111/1750-3841.12539
Zhao, Y., Takhar, P.S., (2017). Micro X-ray computed tomography and image analysis of frozen potatoes subjected to freeze-thaw cycles. *LWT - Food Science and Technology,* 79, 278-286. https://doi.org/10.1016/j.lwt.2017.01.051

List of figures

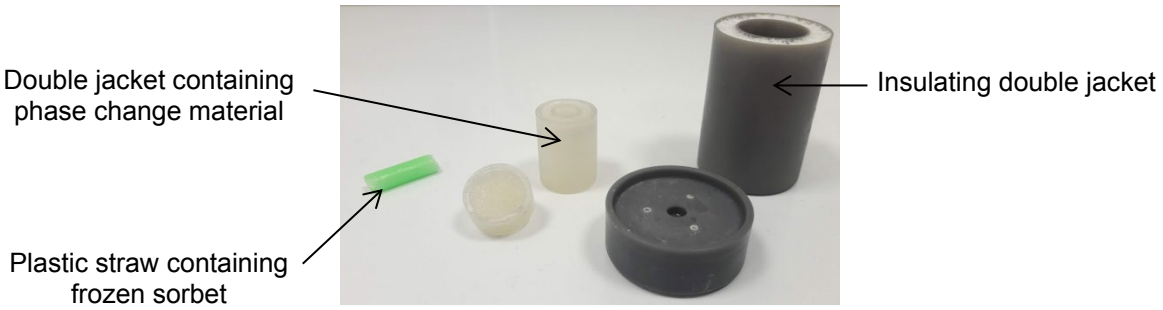
Double jacket containing phase change material
Insulating double jacket
Plastic straw containing frozen sorbet

Figure 1.

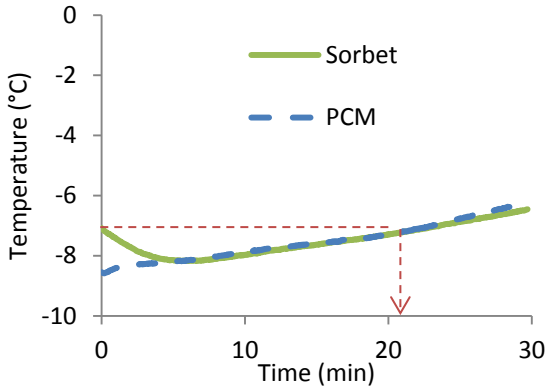

Figure 2.

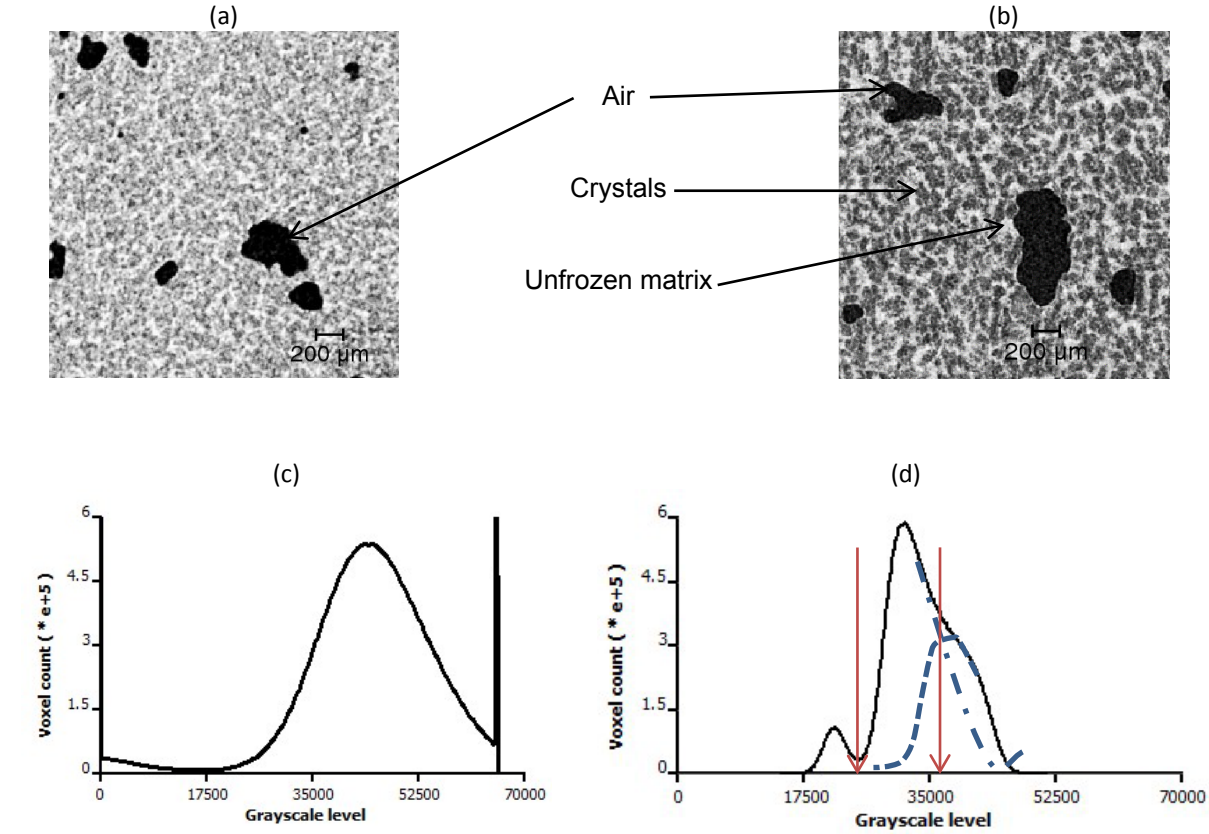
(a)
(b)
Air
Crystals
Unfrozen matrix
200 µm
200 µm
(c)
(d)
Voxel count (* e+5)
Grayscale level
0
1.5
3
4.5
6
0
17500
35000
52500
70000

Figure 3.

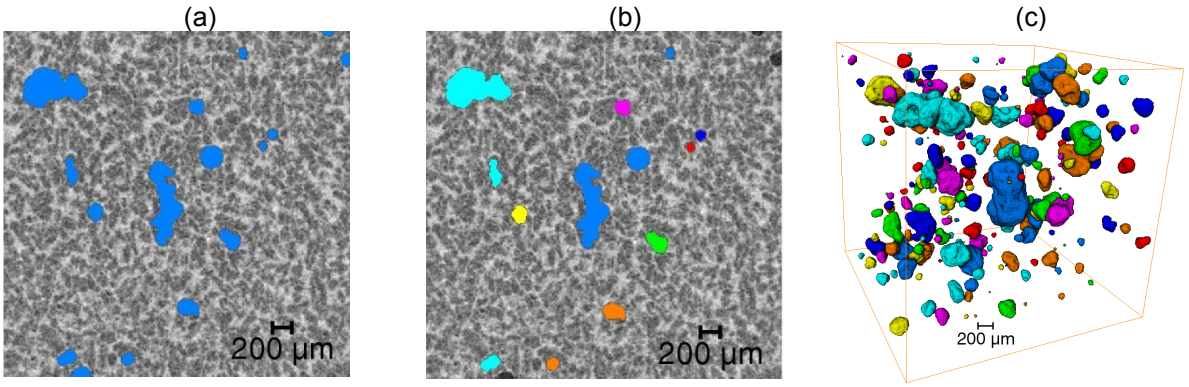

Figure 4.

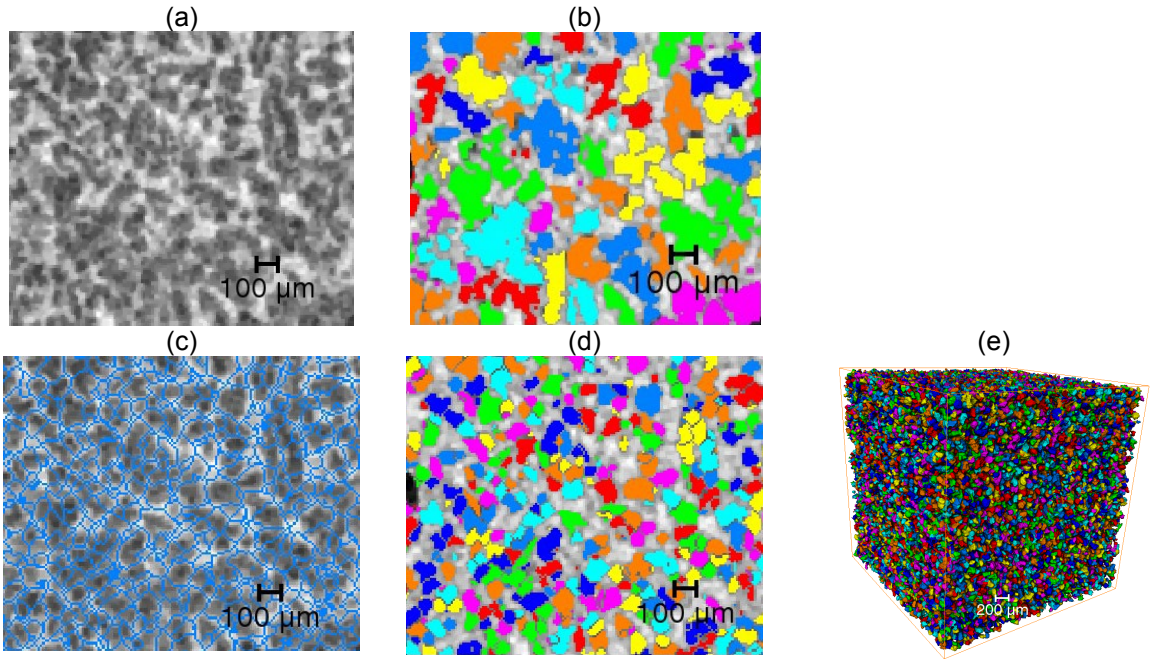

Figure 5.

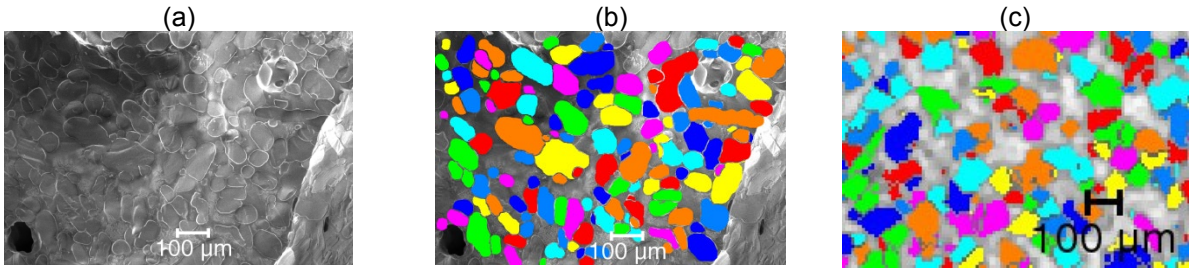

Figure 6.

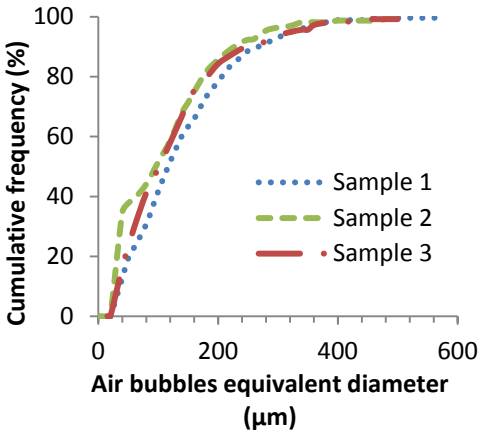
100
80
60
40
20
0
Cumulative frequency (%)
0
200
400
600
Air bubbles equivalent diameter (µm)
Sample 1
Sample 2
Sample 3

Figure 7.

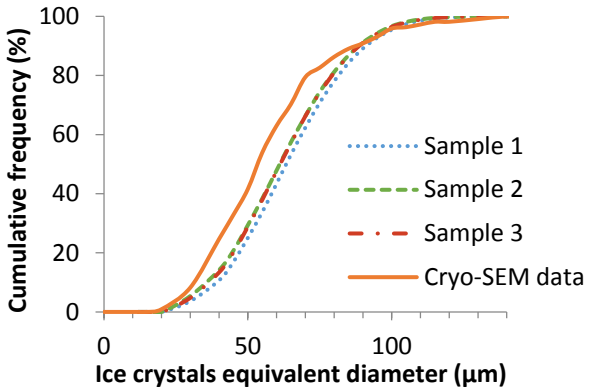
Cumulative frequency (%)
100
80
60
40
20
0
0
50
100
Ice crystals equivalent diameter (µm)
Sample 1
Sample 2
Sample 3
Cryo-SEM data

Figure 8.